INTERNATIONAL JOURNAL OF HYDROGEN ENERGY 34 (2009) 6625–6635

Available at www.sciencedirect.com

ScienceDirect

journal homepage: www.elsevier.com/locate/he

# Bunsen section thermodynamic model for hydrogen production by the sulfur–iodine cycle

Mohamed Kamel Hadj-Kali[a,b], Vincent Gerbaud[a,b,*], Patrick Lovera[c], Olivier Baudouin[d], Pascal Floquet[a,b], Xavier Joulia[a,b], Jean-Marc Borgard[c], Philippe Carles[c]

[a]Université de Toulouse, INP-ENSIACET, UPS, LGC (Laboratoire de Génie Chimique), 4 allée Emile Monso, BP 74233, F-31432 Toulouse Cedex 4, France
[b]CNRS, LGC (Laboratoire de Génie Chimique), 4 allée Emile Monso, F-31432 Toulouse Cedex 4, France
[c]CEA, DEN, Physical Chemistry Department, F-91191 Gif-sur-Yvette, France
[d]ProSim, Stratège Bâtiment A, BP 27210, F-31672 Labège Cedex, France

ARTICLE INFO

*Article history:*
Received 6 April 2009
Received in revised form
8 June 2009
Accepted 9 June 2009
Available online 13 July 2009

*Keywords:*
Sulfur–iodine cycle
Bunsen section
Phase equilibrium modeling
Liquid–liquid equilibrium

ABSTRACT

A model for the Bunsen section of the Sulfur–Iodine thermo-chemical cycle is proposed, where sulfur dioxide reacts with excess water and iodine to produce two demixing liquid aqueous phases ($H_2SO_4$ rich and HI rich) in equilibrium. Considering the mild temperature and pressure conditions, the UNIQUAC activity coefficient model combined with Engels' solvation model is used. The complete model is discussed, with HI solvation by water and by iodine as well as $H_2SO_4$ solvation by water, leading to a very high complexity with almost hundred parameters to be estimated from experimental data. Taking into account the water excess, a successful reduced model with only 15 parameters is proposed after defining new apparent species. Acids total dissociation and total $H^+$ solvation by water are the main assumptions. Results show a good agreement with published experimental data between 25 °C and 120 °C.



## 1. Introduction

Hydrogen is undeniably a very attractive energy carrier, superior to others for power generation, transportation and storage. Nowadays, fossil resources account for 95% of hydrogen production. However, given the prospect of an increasing energy demand, of a shortage of fossil resources and of greenhouse gases release limitation, water could be the only viable and long term candidate raw material for hydrogen production. Electrolysis and thermo-chemical cycles are the two leading processes for massive hydrogen production from water. In thermo-chemical cycles, water is decomposed into hydrogen and oxygen via chemical reactions using intermediate elements which are recycled. As the heat can be directly used, these cycles have the potential of a better efficiency than alkaline electrolysis. For massive hydrogen production, the required energy can be provided either by nuclear energy, by solar energy or by hybrid solutions including both.

Among hundreds of possible cycles, the Sulfur–Iodine (S–I) cycle is a promising one [1] in combination with high temperature heat, having no solid phase under the process operating conditions. The S–I thermo-chemical cycle, depicted in Fig. 1, is divided into three sections, namely: (I) the

* *Corresponding author*. CNRS, LGC (Laboratoire de Génie Chimique), 4 allée Emile Monso, F-31432 Toulouse Cedex 4, France. Tel.: +33 534 323 600.
E-mail address: vincent.gerbaud@ensiacet.fr (V. Gerbaud).
0360-3199/$ – see front matter © 2009 International Association for Hydrogen Energy. Published by Elsevier Ltd. All rights reserved.
doi:10.1016/j.ijhydene.2009.06.022

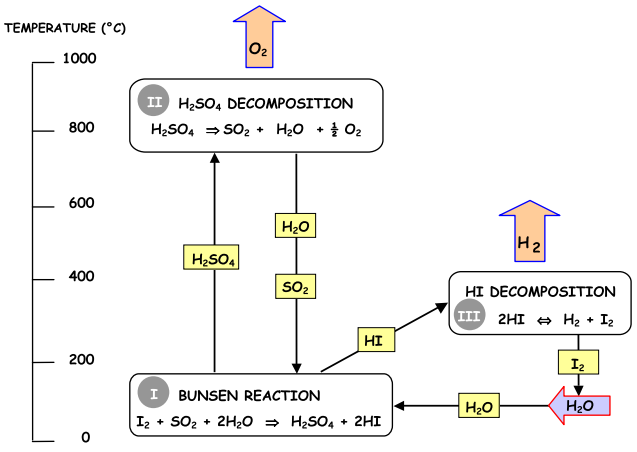


**Fig. 1 – Sulfur–iodine thermo-chemical cycle scheme [1].**

Bunsen section, where water $H_2O$ reacts with iodine $I_2$ and sulfur dioxide $SO_2$ to produce, by using a specific stoichiometry, two immiscible liquid aqueous phases: one phase containing mainly sulfuric acid $H_2SO_4$ and the other phase containing hydroiodic acid (hydrogen iodide) HI and iodine $I_2$ (known as the $HI_x$ phase); (II) the sulfuric acid and (III) the hydrogen iodide concentration and decomposition sections, where intermediate products break down upon heating, releasing hydrogen and oxygen. Water, iodine and sulfur dioxide are recycled in the system [2].

In 2005, Mathias quoted the thermodynamic systems occurring in the Bunsen section and the $HI_x$ section among current challenges for applied thermodynamics [3]. He wrote: "…The sulfuric acid decomposition section of …[the S–I]… process can be simulated accurately, but other sections (acid generation and hydrogen iodide decomposition) illustrate the difficulty of modeling phase behavior, particularly liquid-phase immiscibility, in complex electrolyte systems." Acid generation refers to the Bunsen section.

We have recently proposed a new approach to model the $HI_x$ section [4]: the Peng Robinson equation of state (EoS) approach is supplemented with the MHV2 complex mixing rule that incorporates an Excess Gibbs energy model ($G^{Ex}$) to handle the strong nonideal behavior of the $HI_x$ system. UNIQUAC $G^{Ex}$ model is combined with solvation of hydrogen iodide HI by water $H_2O$ according to Engel's solvation model. In the $HI_x$ section, the resulting EoS/$G^{Ex}$ model is able to describe with accuracy, by using a single set of parameters, all literature vapor–liquid, liquid–liquid, vapor–liquid–liquid and solid–liquid equilibrium data for the $HI_x$ ternary system and the three binary subsystems. Compared to other models for the $HI_x$ system based on an electrolyte model [5–7], the homogeneous EoS/$G^{Ex}$ approach of Hadj-Kali et al. [4] has two major interests: first, it is theoretically compatible with calculations above HI critical temperature, that is likely to occur if a reactive distillation process is chosen for the $HI_x$ section [8–10]. Second, using Engel's solvation model for the solvation of HI by $H_2O$, like Neumann's model [11,12], it is based on a symmetric convention in which the same reference state is supposed for all species, enabling to readily explore equilibrium properties for any composition. Because of a lack of experimental data under the $HI_x$ system conditions, HI dissociation reaction, producing $H_2$ and $I_2$ was not considered [4]. Polyiodide formation in aqueous solution [13–15] was not explicitly considered for the $HI_x$ section but is likely to occur in the Bunsen section, because the milder temperature favors polyiodide formation.

In continuation of the modeling work of the $HI_x$ section, the present paper focuses on the thermodynamic modeling of the Bunsen section. At low pressures, a homogeneous EoS/$G^{Ex}$ approach is not mandatory to model the liquid–liquid equilibrium occurring. We then inspire from the $G^{Ex}$ part of the model of Hadj-Kali et al. [4] by combining the UNIQUAC model with Engel's solvation.

## 2. Background

### 2.1. Bunsen section reactions

#### 2.1.1. Bunsen main reaction

Bunsen main reaction is the following:

$$2H_2O + SO_2 + I_2 \leftrightarrow H_2SO_4 + 2HI \quad \Delta G^\circ(400\ K) = +82\ kJ\ mol^{-1} \quad R1 \tag{1}$$

With $\Delta G^\circ$ being the standard Gibbs free energy. The positive value of $\Delta G^\circ(400\ K)$ implies an extremely small equilibrium constant $K(400\ K) = 1.96 \times 10^{-11}$. Thus the formation of the acids $H_2SO_4$ and HI is not favored unless one of them at least is removed from the reactor. However, according to Le Châtelier's principle, any excess of reactant will be consumed and produce the acids. Indeed iodine in excess favors the production of the acids and the spontaneous demixtion into two aqueous solutions, a light one rich in $H_2SO_4$ (SA phase) and a heavy one rich in HI ($HI_x$ phase). According to Elder et al. [16], the two aqueous phases demixtion arises from the formation of polyiodide ions as iodine ions in the HI phase are solvated by molecular iodine. Besides, water excess enables to dilute both acids with a negative standard Gibbs energy [16]:

$$H_2SO_4 + 4H_2O \leftrightarrow (H_2SO_4 + 4H_2O)_{aq} \quad \Delta G^\circ(400\ K) = -66\ kJ\ mol^{-1} \quad R2 \tag{2}$$

$$2HI + 8I_2 + 10H_2O \leftrightarrow (2HI + 10H_2O + 8I_2)_{aq} \quad \Delta G^\circ(400\ K) = -104\ kJ\ mol^{-1} \quad R3 \tag{3}$$

Therefore, the overall reaction is (R1) + (R2) + (R3) and General Atomics [17] proposed the typical equation for the Bunsen process:

$$9I_2 + SO_2 + 16H_2O \leftrightarrow (2HI + 10H_2O + 8I_2)_{aq} + (H_2SO_4 + 4H_2O)_{aq} \quad R4 \tag{4}$$

This reaction strongly favors the production of the aqueous acid phases as its standard Gibbs energy equals $\Delta G^\circ(400\ K) = -88\ kJ\ mol^{-1}$, leading to an equilibrium constant value $K(400\ K) = 3.1 \times 10^{11}$.

Finally, Kracek [18] observed that below 493 K, $H_2O$–$I_2$ binary mixture has a very large immiscibility gap between

approximately $nH_2O/nI_2 \in \{0.03; 99\}$, encompassing both water–iodine molar ratio in reaction R1 ($nH_2O/nI_2 = 2$) or R4 ($nH_2O/nI_2 = 1.78$ for the reactants, $nH_2O/nI_2 = 1.75$ for the products) and thus likely explaining why demixtion occurs.

#### 2.1.2. *Bunsen section side reactions*

Side reactions occur in the Bunsen section to produce sulfur S and hydrogen sulfide $H_2S$ [19]:

$$6HI + H_2SO_4 \leftrightarrow S + 3I_2 + 4H_2O \quad R5 \tag{5}$$

$$8HI + H_2SO_4 \leftrightarrow H_2S + 4I_2 + 4H_2O \quad R6 \tag{6}$$

Sakurai et al. [19] studied in HI, $H_2SO_4$ and $I_2$ solutions the concentration and temperature conditions under which those side reactions occur: reaction R6 is favored between 295 K and 368 K over reaction R5, the opposite under low iodine excess; both equations are overall enhanced by a higher temperature, higher acid concentrations and low iodine excess. They suggest that operating at 368 K requires to control iodine concentration so that poly hydroiodic ($HI_x$) acids is above $x = 4.41$ to avoid side reactions and below $x = 11.99$ to prevent iodine crystallization.

#### 2.1.3. *Polyiodides formation*

The solvation power of iodine is well known and quite similar to water solvation. Palmer and Lietzke [13] have studied the kinetics and equilibria of iodine hydrolysis. They postulated the existence of $I^-$, $I_3^-$, $I_2O^-$, $OI^-$ ions, giving for each one a mathematical expression of the equilibrium constant, while discarding $I_5^-$ and $I_6^{2-}$ ions regarding their low iodine concentration during the experiments. The following reaction illustrates the polyiodides formation:

$$MI + I_2 \Leftrightarrow MI_3 \quad \text{or} \quad I^- + I_2 \Leftrightarrow I_3^- \quad R7 \tag{7}$$

with

$$T \cdot \ln K = 3727.86 - 11.6326 \cdot T + 0.019221 \cdot T^2 \tag{8}$$

Calabrese and Khan [15] also identified $I_3^-$ and several polyiodide ions $I_{2x}H^+$ (with $x = 2, 3$, etc.) in aqueous solutions of KI where iodine is introduced. Again, they discard $I_5^-$ and $I_7^-$ ions regarding the low iodine content introduced. The equilibrium constant expression (equation (8)) suggests that $I_3^-$ is favored at the temperature expected for the Bunsen section.

### 2.2. *Liquid–liquid equilibrium experimental data*

Two experimental approaches are considered. The first mixes Bunsen reaction's three reactants ($SO_2$, $I_2$ and $H_2O$) at various temperatures and explores in so-called 1/*m*/*n* data points the impact of *m* or *n* molecules of iodine or water reacting with $SO_2$. General Atomic typical stoichiometry of reaction R4 corresponds to a 1/9/16 data point.

The second approach mixes the four reaction products, $H_2SO_4$, HI, $I_2$ and $H_2O$ at various temperatures and explores in so-called 1/*a*/*b*/*c* data points the impact of HI (*a*), $I_2$ (*b*) and $H_2O$ (*c*) mole number in contact with one sulfuric acid mole. General Atomic typical stoichiometry of reaction R4 corresponds to a 1/2/8/14 data point. Usually iodine content has a lower limit to ensure liquid–liquid-phase split and an upper one to avoid iodine precipitation.

Sakurai et al. [20,21] have analysed the influence of temperature and iodine for various initial mixtures $H_2SO_4$/HI/$H_2O$ = 0.048/0.070/0.882 (at 273, 301, 313, 333, 353 and 368 K), $H_2SO_4$/HI/$H_2O$ = 0.058/0.085/0.857 (at 313 K), $H_2SO_4$/HI/$H_2O$ = 0.069/0.049/0.882 (at 313 K). Among their conclusions, they noticed that the impurity content in each phase (i.e. $H_2SO_4$ in $HI_x$ phase and $I_2$ together with HI in SA phase) decreases as the iodine content increases. They also noticed that under iodine saturation conditions, separation at 368 K enables to reduce by 25% impurities in the $HI_x$ phase and by 20% in the SA phase. Experimental data accuracy is not known.

Kang et al. [22] carried out a large set of experiments between 298 K and 393 K for 1/2/0.5–8/14–20 data points. The lowest impurities are achieved at 353 K with the highest iodine content. They also notice that excess water has more affinity with the $HI_x$ phase than with the SA phase, but that this affinity decreases with temperature and increases with iodine molar fraction.

Giaconia et al. [23] published 1/2/4–16/11.2–15.8 data points from 353 K to 393 K. They concluded that the temperature and iodine content did not affect much the HI and $H_2SO_4$ split among the $HI_x$ phase and the SA phase. They also noticed that high iodine content reduced impurities in both phases and that excess water goes into the SA rich phase. Accuracy is claimed to be 0.002 molar fraction for HI and $I_2$ in the SA phase and 0.01 molar fraction for all other species in the SA and $HI_x$ phase.

Lee et al. [24] have reviewed the aforementioned literature Bunsen section liquid–liquid equilibrium experimental data in terms of 1/*a*/*b*/*c* data points, including other Korean data points from a Master's thesis (see [24]). They have combined them in a database of 69 data points to highlight the temperature, HI content and excess iodine and water in the feed. This database is consistent despite the absence of accuracy data and is used as a reference in the present work.

### 2.3. *Bunsen section thermodynamic and former models*

#### 2.3.1. *Liquid–liquid equilibrium*

Liquid–liquid equilibrium are computed from the usual thermodynamic condition, activities equality:

$$a_i(T, \mathbf{x}) = a_i(T, \mathbf{x}') \quad \text{or} \quad \gamma_i(T, \mathbf{x}) \cdot x_i = \gamma_i(T, \mathbf{x}') \cdot x_i' \tag{9}$$

It then requires an excess Gibbs energy model to compute the activities $a_i$ or the activity coefficients $\gamma_i$.

#### 2.3.2. *Nonideal solution behavior: former thermodynamic models*

Bunsen section compounds form a strongly nonideal mixture. Occurrence of strong acids like HI and $H_2SO_4$ in aqueous solutions hints at the occurrence of electrolytes, well known to interact over long range. The nonideal behavior could be handled using an excess Gibbs energy model.

Literature models on the Bunsen section are scarce and not fully satisfying.

Davis and Conger [25] proposed an electrolytic activity coefficient model based on a Pitzer–Debye–Hückel approach. They describe the sulfuric and hydroiodic acid phases by the dissociation equations relative to $H_2SO_4$, $SO_2$, and water, and to HI, $SO_2$ and water respectively. Therefore, they imply that

$H_2SO_4$ is found only in the SA phase and HI only in the $HI_x$ phase. They validate the model on a single experimental point with initial $nH_2O/nI_2 = 2.0713$ at 368 K. Their results underestimate the water quantity in the SA phase and thus overestimate it in the $HI_x$ phase.

Mathias [26] used the electrolyte-NRTL model developed by Chen et al. [27,28] that combines the Pitzer–Debye–Hückel model [29] for long-range ion–ion electrostatic interactions with the NRTL theory [30] for short-range energetic interactions among the species in electrolyte solutions. The reactions considered are:

$$H_2SO_4 + H_2O \leftrightarrow H_3O^+ + HSO_4^- \tag{10}$$

$$HI + H_2O + 1/4I_2 \leftrightarrow \{HI_x \text{aqueous phase}\} \tag{11}$$

Mathias indicates that iodine and HI form the complex $HI_x$ in aqueous solutions, of which exact composition "x" should be determined to best describe experimental data.

Recently, O'Connell [31] hinted at a possible improvement of Mathias' approach by considering the two reactions:

$$HI + 4H_2O \leftrightarrow H_3O^+ + I^-, (H_2O)_3 \tag{12}$$

$$HI + 2I_2 \leftrightarrow I_2H^+ + I_3^- \tag{13}$$

No consistent results are provided though.

Those electrolyte models are based on an asymmetric convention for the electrolyte and the solvent which does not allow their application over the entire composition range [32]. Chen's electrolyte-NRTL model claims accurate prediction of activity coefficient up to 16 mol $kg^{-1}$ of solvent for strong acid electrolytes like HCl or $H_2SO_4$ [33].

## 3. Bunsen section new thermodynamic model

We propose to combine the UNIQUAC model for nonideal interactions phenomena with Engel's solvation model for long range electrolytic interaction phenomena. A similar approach was used successfully alone and into the MHV2 complex mixing rule applied to the Peng Robinson equation of state to model the $HI_x$ section thermodynamics [4].

However, application to the Bunsen section phenomena rapidly leads to an unsolvable complexity, which hinted us at devising a simplified representation of the phenomena.

### 3.1. *Thermodynamic model*

#### 3.1.1. *Nonideal interaction model: UNIQUAC*

The local composition model UNIQUAC is based on a symmetric convention for all species. UNIQUAC sums a combinatorial term accounting for the entropic contribution and a residual term accounting for intermolecular interactions, responsible for the mixing enthalpy [34].

$$\frac{G^{Ex}}{RT} = \left(\frac{G^{Ex}}{RT}\right)_{\text{combinatorial}} + \left(\frac{G^{Ex}}{RT}\right)_{\text{residual}} = f_{\text{combinatorial}}(\mathbf{x}, r, q) + f_{\text{residual}}(\mathbf{x}, q', A_{ij}, A_{ji}) \tag{14}$$

The activity coefficient expression is:

$$Ln\,\gamma_i = \left(Ln\frac{\phi_i}{x_i} + \frac{z}{2}q_i\,Ln\frac{\theta_i}{\phi_i} + l_i - \frac{\phi_i}{x_i}\sum_{j=1}^{n} x_j l_j\right) + \left(q_i' - q_i'\,Ln\left(\sum_{j=1}^{n}\theta_j\tau_{ji}\right) - q_i'\sum_{j=1}^{n}\frac{\theta_j'\tau_{ij}}{\sum_{k=1}^{n}\theta_k'\tau_{kj}}\right) \tag{15}$$

with:

$\tau_{ij} = \exp - (A_{ij}/RT)$, $\tau_{ii} = \tau_{jj} = 1$, $l_i = z/2(r_i - q_i) - (r_i - 1)$, $z = 10$.

$$\phi_i = \frac{x_i r_i}{\sum_j x_j r_j} \quad \theta_i = \frac{x_i q_i}{\sum_j x_j q_j} \quad \theta_i' = \frac{x_i q_i'}{\sum_j x_j q_j'}$$

Binary interaction parameters $A_{ij}$ and $A_{ji}$ (in cal/mol) are estimated from experimental data, considering a temperature linear dependency:

$$A_{ij} = A_{ij}^0 + A_{ij}^T T \tag{16}$$

Parameters $r_i$, $q_i$ and $q_i'$ are molecular constants that can be estimated for any new species, like solvation complexes, using the group contribution method of Bondi [35], as suggested by UNIQUAC author's [34,36].

#### 3.1.2. *Long range electrolytic interactions: Engels' solvation model*

An alternative model for electrolytes is provided by Engels solvation model, based on the concept that ions exist in solution only within a stable solvent cloud [37]. The new molecule clusters called "complexes" C are made by the reaction of $m$ solvent molecules S with one electrolyte E molecule according to the expression:

$$mS + E \leftrightarrow \upsilon C \quad K = \frac{a_C^\upsilon}{a_E \times a_S^m} = \frac{\gamma_C^\upsilon}{\gamma_E \times \gamma_S^m} \times \frac{x_C^\upsilon}{x_E \times x_S^m} \tag{17}$$

Where $\upsilon$ is the number of dissociation products of one electrolyte molecule; $x_i$ is the molar fraction of the species i and $a_i$, $\gamma_i$ their activity and activity coefficient respectively. $K$ is the solvation constant with a temperature dependency like:

$$K = \exp(A_K + B_K/T) \tag{18}$$

where $A_K$ and $B_K$ are the solvation constant parameters.

This model uses a symmetric convention for both the electrolyte and the solvent, removing any limitation over the composition range. Under dilute electrolyte conditions, the excess of solvent favors the complete dissociation and solvation of the electrolyte. Near pure electrolyte, lack of solvent leaves the electrolyte undissociated. For $H_2O$–HI mixtures, this is consistent with solid–liquid equilibrium data [38] showing a decrease in the hydration number in solid HI, $nH_2O$ as water composition decreases.

Equation (17) results from the strict thermodynamic description of an electrolyte dissociation followed by solvation of the cation. For example, for $H_2O$–HI, we write:

$$HI \leftrightarrow H^+ + I^- \quad K_a = \frac{a_{H^+}a_{I^-}}{a_{HI}} \tag{19}$$

$$mH_2O + H^+ \leftrightarrow \left[H_3O^+, (m-1)H_2O\right] \quad K_{H^+\text{solvation}} = \frac{a_{(H_3O^+,(m-1)H_2O)}}{a_{H^+}a_{H_2O}^m} \tag{20}$$

$$mH_2O + HI \leftrightarrow [H_3O^+, (m-1)H_2O] + I^- \quad (21)$$
$$K = \frac{a_{I^-} a_{(H_3O^+,(m-1)H_2O)}}{a_{HI} a_{H_2O}^m} = \frac{a_C^2}{a_{HI} a_{H_2O}^m}$$

The equilibrium constant of equations (17) and (21) are equivalent with a complex 2C that would be like $\{[H_3O^+,(m-1)H_2O]; I^-\}$. Writing of $H_3O^+$ is based on hydronium ion evidence in aqueous solutions, with a hydration number that may vary upon conditions [39].

Engels' model was first used successfully by its author with the Wilson activity coefficient model [37] to describe the vapor–liquid-phase equilibrium of the binary mixture $H_2O$–HI. It was also successfully used in several thermodynamic approaches of the $HI_x$ section in the Sulfur–Iodine thermo-chemical cycle, by Neumann [11], Yoon et al. [12] and Hadj-Kali et al. [4] to account for HI solvation by water.

### 3.2. Bunsen section complete model

One of the challenges of the Bunsen section is to investigate how much excess water and iodine can be reduced so as to limit the recycle flowrates, without impeding the two acid phase production by reaction R1 or R4 and maintaining side reactions R5 and R6 under control. However, based on the information available in Lee's data compilation, we restrict ourselves to consider the Bunsen forward reaction, discarding $SO_2$, S or $H_2S$ species.

At first the UNIQUAC + Engels solvation model can handle the following phenomena:

1. Liquid–liquid equilibrium between the SA phase and the $HI_x$ phase.
2. Solvation of HI by $H_2O$ ($HI_x$ phase):

$$m_1H_2O + HI \leftrightarrow 2C_1 \quad \text{with } \{2C_1\} \equiv \{[H_3O^+, (m_1-1)H_2O]; I^-\} \quad (RS1) \quad (22)$$

3. Solvation of first acidity of $H_2SO_4$ by $H_2O$ (SA phase):

$$m_2H_2O + H_2SO_4 \leftrightarrow 2C_2 \quad \text{with } \{2C_2\} \equiv \{[H_3O^+, (m_2-1)H_2O]; HSO_4^-\} \quad (RS2) \quad (23)$$

4. Solvation of HI by $I_2$ in the presence of water ($HI_x$ phase):

$$m_1H_2O + m_3I_2 + HI \leftrightarrow 2C_3 \quad \text{with } \{2C_3\} = \{[H_3O^+, (m_1-1)H_2O]; [I_3^-, (m_3-1)I_2]\} \quad (RS3) \quad (24)$$

Therefore, there are $n = 7$ true species: $I_2$, HI, $H_2O$, $H_2SO_4$, C1, C2 and C3 with 93 parameters requiring estimation: 84 parameters, $A_{ij}^0$, $A_{ji}^0$, $A_{ij}^T$ and $A_{ji}^T$ for the calculation of the $n(n-1)$ binary interactions $A_{ij}$ et $A_{ji}$ from equation (16); 2 parameters $A_K$ and $B_K$ for each three solvation constant and, finally, three solvation numbers, $m_1$, $m_2$, $m_3$.

### 3.3. Bunsen section simplified representation

#### 3.3.1. Measured, apparent and true species

The analysis of literature experimental data [19,21,23,24] shows that the measured molar ratio $nH_2O/nHI$ and $nH_2O/nH_2SO_4$ is always greater than 3 in the initial composition or in the two equilibrium SA and $HI_x$ aqueous phases composition. We take advantage of the water excess in the following hypotheses.

*3.3.1.1. Hypothesis of acid total dissociation in excess water.* Considering the HI dissociation constant in aqueous solution ($pK_a = -\log_{10}K_a = -10$ at 298 K), we postulate that HI is fully dissociated. The same is assumed for the first acidity of $H_2SO_4$ ($pK_{a1} = -3$ at 298 K):

$$H_2SO_4 \rightarrow H^+ + HSO_4^- \quad (25)$$

The second acidity ($pK_{a2} = 1.99$ at 298 K) is neglected.

*3.3.1.2. Hypothesis of $H^+$ ion solvation by three water molecules.* All $H^+$ ions are supposed to be solvated by three $H_2O$ molecules, independently whether they come from HI or $H_2SO_4$ total dissociation ($m_1 = m_2 = 3$ in equations (21) and (22)).

Those last two hypotheses enable to substitute the measured species HI and $H_2SO_4$ by two apparent species, that we write $[H_2SO_4, 3H_2O]$ and $[HI, 3H_2O]$. These apparent species correspond to the complexes $\{[H_3O^+, (m_2-1)H_2O]; HSO_4^-\}$ and $\{[H_3O^+,(m_1-1)H_2O]; I^-\}$.

Molar fractions of apparent species are computed from mass balances, accounting for the fact that apparent, or free, water now equals to the measured water minus the water used for the hydration of HI and $H_2SO_4$:

*3.3.1.3. Hypothesis of hydrated HI acid solvation by iodine.* To cope with the occurrence of polyiodides $[I^-,m_3I_2]$ in aqueous solution [13–15], each hydrated complex $[HI, 3H_2O]$ is solvated by $m_3$ moles of iodine in excess following Engels' solvation model:

$$[HI, 3H_2O] + m_3I_2 \leftrightarrow 2C_3 \quad (26)$$

Furthermore, we postulate that $m_3 = 1$. So, $\{2C_3\}$ is also equivalent to $\{[H_3O^+, 2H_2O]; I_3^-\}$.

Together, these hypotheses lead to define four apparent species, $I_2$, free $H_2O$, $[HI, 3H_2O]$ and $[H_2SO_4, 3H_2O]$, and five true species when the $\{2C_3\}$ species is added. With five species, the number of parameters to identify reduces from 84 binary parameters to 40 and from 9 solvation parameters to 2. True species molar fractions are computed from mass balances and the solvation equilibrium equation (26).

In spite of these first level hypotheses, the total number of parameters of this simplified model, equal to 42, remains too much in front of the available experimental data. It is why a second level set of hypothesis must be formulated.

#### 3.3.2. True species interaction matrix

We further postulate that $[H_2SO_4, 3H_2O]$ hydrated complex interacts like water with other species. Indeed, modeling of $H_2O$–$H_2SO_4$ binary mixtures vapor–liquid equilibrium using Engels' proposal [37] shows that the interaction between water and the $\{2C_2\}$ solvation complex of $H_2SO_4$ by $H_2O$ (see equation (23)) is negligible. By doing so, we consider that the chemical theory alone allow to represent the nonideal behavior of the solution.

Finally, we postulate that the new solvation complex $\{2C_3\}$ of [HI, $3H_2O$] by $I_2$ behaves like $I_2$ and that their binary interaction is null.

The true species binary interaction parameter matrix (see Table 1) becomes:

The number of binary parameters, $A_{ij}^0$, $A_{ji}^0$, $A_{ij}^T$ and$A_{ji}^T$, reduces to 12 plus the 2 parameters $A_K$ and $B_K$ of the $\{C_3\}$ solvation constant. The solvation number $m_3$ is set to unity.

Interactions between $H_2O$ and $I_2$ are initialised on the basis of liquid–liquid equilibrium data of Kracek [18] as done in a previous study [4].

The new species [HI, $3H_2O$], [$H_2SO_4$, $3H_2O$] and $\{2C_3\} \equiv \{[H_3O^+, 2H_2O]; I_3^-\}$ are created in Simulis® Thermodynamics thermophysical properties calculation server [40] and their UNIQUAC parameters $r_i$, and $q_i$ estimated according to Bondi's group contribution method [35].

## 4. Results

### 4.1. Data analysis

- The model parameters are estimated on the basis of the 45 of the 50 Korean points (K01–K50) among the 69 $H_2SO_4$/HI/$I_2$/$H_2O$ data points combined by Lee et al. [24] covering temperatures from 298.15 K to 393.15 K. Lee et al. reported Giaconia and coworker's "point entry 5" [23] at a temperature of 368.5 K instead of 393.5 K. We corrected Lee's G06 accordingly. The remaining points from Giaconia (G01–G10) and from Sakurai (S01–S09) are used for validation only.
- Among the 69 experimental data points, 67 have enough water, globally and in both acid phases to ensure that apparent species [$H_2SO_4$, $3H_2O$], [HI, $3H_2O$], $I_2$, $H_2O$ molar fractions are physically coherent, that means positive. Indeed, experimental points G04 and G06 lack water in the $HI_x$ phase to hydrate HI and $H_2SO_4$ with 3 $H_2O$ in this phase. However, the water missing is very small and for these points the free water molar fraction in the $HI_x$ phase is considered null for the purpose of calculating apparent species molar fraction.
- Experimental points G02 and G05 contain exactly enough water in the $HI_x$ phase to hydrate HI and $H_2SO_4$ with 3 $H_2O$ in this phase. The free water molar fraction is therefore null.
- Experimental points K19 and K38 show a suspiciously low $H_2SO_4$ molar fraction in the $HI_x$ phase (0.003 and 0.008), compared to surrounding measures at the same temperature all at least twice greater.
- Experimental points K29, K40, K41, K42, K47, K48, K49, K50 of Lee et al. [24] show a zero molar fraction for impurity $I_2$ in the SA phase at temperature of 373.15 K and 393.15 K. Experimental points S09, G02, G05, G10 of Sakurai and Giaconia are alike.
- Molar fraction data show that in phase SA, $I_2$ and HI are impurities whereas $H_2O$ and $H_2SO_4$ are the main species. In phase $HI_x$, $H_2SO_4$ is the impurity whereas $H_2O$, $I_2$, and HI are the main species.
- Points K09, K14, K35, K36, K43 are the only points with a molar ratio $nI_2/nH_2SO_4$ lower than unity. They are excluded from the parameter estimation procedure.

### 4.2. Parameter estimation criterion

We use a relative least square criterion to enhance the weight of impurities molar fractions in the estimation procedures. The null molar fraction values are included in the criterion calculation by dividing the absolute error ($x^{exp} - x^{calc}$) by 0.001.

$$\text{Criterion} = \frac{1}{N'} \sum_{\varphi=1}^{HI_x,SA\ phases} \left( \sum_{i=1}^{apparent\ species} \left( \sum_{j=1}^{N} \left( \frac{x_{i,j,\varphi}^{exp} - x_{i,j,\varphi}^{calc}}{x_{i,j,\varphi}^{exp}} \right)^2 \right) \right) \tag{27}$$

$N$ is the number of points in each phase and $N'$ is the total number of points.

### 4.3. Parameter set

Table 2 displays the binary interaction parameters for the true species and the parameters of the solvation constant of the Bunsen section simplified model.

Evidently, there is a strong correlation between the $I_2$ – [HI, $3H_2O$] binary parameters and the [HI, $3H_2O$] by $I_2$ solvation constant parameters. They are both used to balance the species repartition between iodine, hydrogen iodide (through [HI, $3H_2O$]) and polyiodides (through the complex $\{2C_3\}$) in the mixtures. Solvation belongs to a chemical modeling approach; binary interaction parameters rather belong to a physical modeling approach. We experienced that both approaches are needed for the Bunsen section mixtures.

### 4.4. Discussion

Table 3 reports the mean and median relative errors on the experimentally measured molar fractions for all species, for all impurity species in both phases and for the main species in both phases. The values are also displayed for each of the six temperatures spanned by the Korean data used for the estimation of the parameters displayed in Table 2. Data of Sakurai et al. [20,21] and Giaconia et al. [23] are not used in the parameter estimation procedure but as validation of the model through their recording in Lee's table [24]. The median is also displayed, as being less influenced by extreme values.

Apparent species error values that were used in the procedure are not directly meaningful with respect to the

**Table 1 – True species binary interaction parameter matrix.**

| | $I_2$ | $\{2C_3\}$ | $H_2O$ | [$H_2SO_4$, $3H_2O$] | [HI, $3H_2O$] |
|---|---|---|---|---|---|
| $I_2$ | | 0 | | $A_{12}$ | $A_{13}$ |
| $\{2C_3\}$ | | | | | |
| $H_2O$ | | $A_{21}$ | | 0 | $A_{23}$ |
| [$H_2SO_4$, $3H_2O$] | | | | | |
| [HI, $3H_2O$] | | $A_{31}$ | | $A_{32}$ | 0 |

**Table 2 – Parameters of the Bunsen section simplified model.**

| $i$ | $j$ | $A_{ij}^{\circ}$ (K) | $A_{ji}^{\circ}$ (K) | $A_{ij}^{T}$ (K) | $A_{ji}^{T}$ (K) |
|---|---|---|---|---|---|
| $I_2$ | [HI, $3H_2O$] | 19.836 | −387.468 | 0.050 | 0.886 |
| $I_2$ | $H_2O$ | 327.019 | −1132.212 | −1.474 | 6.491 |
| $I_2$ | [$H_2SO_4$, $3H_2O$] | 327.019 | −1132.212 | −1.474 | 6.491 |
| $I_2$ | {$2C_3$} | 0.000 | 0.000 | 0.000 | 0.000 |
| [HI, $3H_2O$] | $H_2O$ | −185.305 | 35.224 | 0.010 | 0.735 |
| [HI, $3H_2O$] | [$H_2SO_4$, $3H_2O$] | −185.305 | 35.224 | 0.010 | 0.735 |
| [HI, $3H_2O$] | {$2C_3$} | −387.468 | 19.836 | 0.886 | 0.050 |
| $H_2O$ | [$H_2SO_4$, $3H_2O$] | 0.000 | 0.000 | 0.000 | 0.000 |
| $H_2O$ | {$2C_3$} | −1132.212 | 327.019 | 6.491 | −1.474 |
| [$H_2SO_4$, $3H_2O$] | {$2C_3$} | −1132.212 | 327.019 | 6.491 | −1.474 |
| | $A_K$ | $B_K$ (K) | | | |
| $K$ (eq. (24)) | −1.270 | 850.000 | | | |

experimentally measured data. Thus, they are not reported but can be obtained from the authors upon request.

#### 4.4.1. *Liquid–liquid-phase splitting*

First, regarding liquid–liquid-phase splitting, the 45 data points taken in the parameter estimation procedure demix according to the model's predictions. Sakurai's {S01–S09} points and Giaconia's {G01–G10} points also demix. The 5 points with $nI_2/nH_2SO_4 < 1$ {K09; K14; K24; K35–K36; K43} do not demix, another reason for which we excluded them from the procedure. Kang et al. [22] also published four points where they reported no demixtion. The model predicts correctly Kang's observations.

#### 4.4.2. *Deviation of the model from Lee's data points*

Regarding the parameter estimation on Lee's data points, Table 3 shows that the relative error is quite small for the main species, either the mean one equal to 5.8% or the median one to 2.9%. It is greater for the so-called impurity species, with the mean one equals to 27.5 % and the median one to 29.5%. This is due to the fact that relative errors are always large for small experimental molar fractions as those of impurities. Overall, for all species, the mean relative error (17.1%) and the median one (5.4%) are quite reasonable. Besides, according to Table 3, there are no significant differences between the various temperature sets, hinting at a reasonable temperature dependency of the parameters.

Table 4 reports the median, mean and maximum relative errors for each experimentally measured species in each phase.

A closer look at each species (Table 4) shows that in each phase the errors related to the main species are quite low, the largest being observed for $H_2SO_4$ in the SA phase. For the impurity species, Table 4 shows that $I_2$ in the SA phase bears the greatest relative errors, being also the smallest impurity molar fraction.

Mean and median are alike, indicating no significantly large error, as it is confirmed by the moderate maximum error values.

The two suspicious $H_2SO_4$ molar fractions in the $HI_x$ phase (K19 and K38 points) that are 0.0030 and 0.0080 molar fractions are computed as 0.0087 and 0.0104 respectively, larger values, in better accordance regarding the surrounding data points.

Experimental and calculated data values are displayed for the impurities and main component in the $H_2SO_4$-rich phase and in the in the HI-rich phase. K09, K14, K35, K36, K43 data points are excluded for the reasons explained before. +10% and −10% error lines are displayed for indication. Fig. 2 concerns 25 °C and 40 °C temperatures; Figs. 3 and 4 concerns 60 °C and 80 °C temperatures; Fig. 2 concerns 100 °C and 120 °C temperatures.

First, we notice that in the $H_2SO_4$-rich phase the model underestimate the molar fractions of the impurities HI and $I_2$ at 25 °C and $I_2$ at 40 °C. Other molar fractions are reasonably well predicted, in particular the $H_2SO_4$ impurity in the HI-rich phase. We do not understand why the underestimation does

**Table 3 – Criterion, mean and median relative errors on experimentally measured species for the Bunsen section simplified model upon the data of Lee et al. [24]; data of Sakurai and Giaconia in Lee et al. [24].**

| | All species | | Impurities | | Main species | |
|---|---|---|---|---|---|---|
| | Mean | Median | Mean | Median | Mean | Median |
| *Estimation* | | | | | | |
| Lee 25 °C | 13.5% | 3.4% | 30.5% | 30.6% | 3.3% | 1.9% |
| Lee 40 °C | 17.1% | 6.6% | 32.7% | 18.2% | 7.7% | 3.1% |
| Lee 60 °C | 20.0% | 9.9% | 41.9% | 30.2% | 6.9% | 3.7% |
| Lee 80 °C | 16.0% | 7.3% | 31.8% | 27.1% | 6.5% | 3.3% |
| Lee 100 °C | 20.5% | 7.6% | 45.6% | 37.8% | 5.5% | 1.6% |
| Lee 120 °C | 15.9% | 4.2% | 33.2% | 27.9% | 5.6% | 1.5% |
| Lee 25 – 120 °C | **17.1%** | **5.4%** | **27.5%** | **29.5%** | **5.8%** | **2.9%** |
| *Validation* | | | | | | |
| Sakurai | 26.4% | 15.7% | 51.6% | 55.2% | 11.2% | 7.4% |
| Giaconia | 36.3% | 14.8% | 71.8% | 32.8% | 15.1% | 12.4% |

**Table 4 – Species mean and median relative errors on experimentally measured species for the Bunsen section simplified model upon the data of Lee et al. [24]; data of Sakurai and Giaconia in Lee et al. [24].**

| | Upper $H_2SO_4$-rich phase | | | | Lower HI rich phase | | | |
|---|---|---|---|---|---|---|---|---|
| | $I_2$[a] | HI[a] | $H_2O$ | $H_2SO_4$ | $I_2$ | HI | $H_2O$ | $H_2SO_4$[a] |
| *Estimation* | | | | | | | | |
| Lee 25 – 120 °C | | | | | | | | |
| Mean | 61.0% | 21.0% | 1.9% | 15.6% | 5.2% | 5.9% | 2.8% | 34.6% |
| Median | 62.5% | 14.7% | 1.4% | 9.5% | 3.7% | 4.9% | 2.6% | 27.9% |
| Max | 94.3% | 78.8% | 5.5% | 68.4% | 21.0% | 19.2% | 7.1% | 69.3% |
| *Validation* | | | | | | | | |
| Sakurai | | | | | | | | |
| Mean | 73.9% | 45.8% | 2.7% | 16.4% | 24.1% | 25.1% | 10.7% | 39.0% |
| Median | 82.1% | 54.5% | 2.5% | 15.3% | 24.1% | 22.1% | 6.9% | 41.2% |
| Max | 94.0% | 68.5% | 3.7% | 25.3% | 33.3% | 54.9% | 21.3% | 66.6% |
| Giaconia | | | | | | | | |
| Mean | 47.2% | 16.4% | 4.8% | 28.3% | 9.2% | 7.2% | 7.9% | 68.8% |
| Median | 48.3% | 6.8% | 5.8% | 35.4% | 9.7% | 7.1% | 8.4% | 18.1% |
| Max | 67.2% | 42.3% | 7.8% | 44.5% | 17.2% | 14.7% | 11.0% | 494.1% |

a Impurity species.

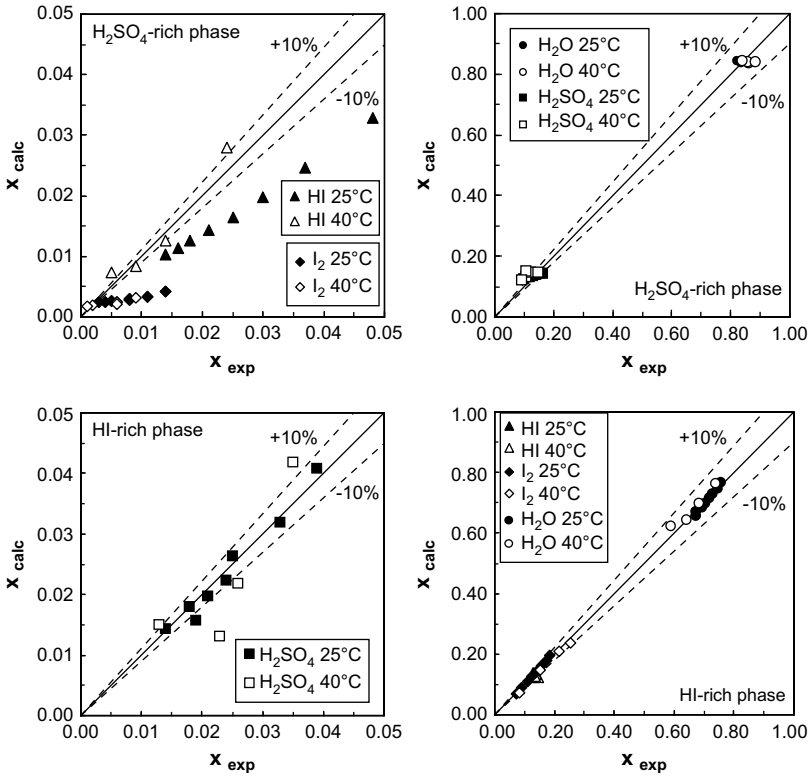


**Fig. 2 – Comparison of experimental and calculated values for Korean data points at 25 °C and 40 °C reported in Lee et al. [24].**

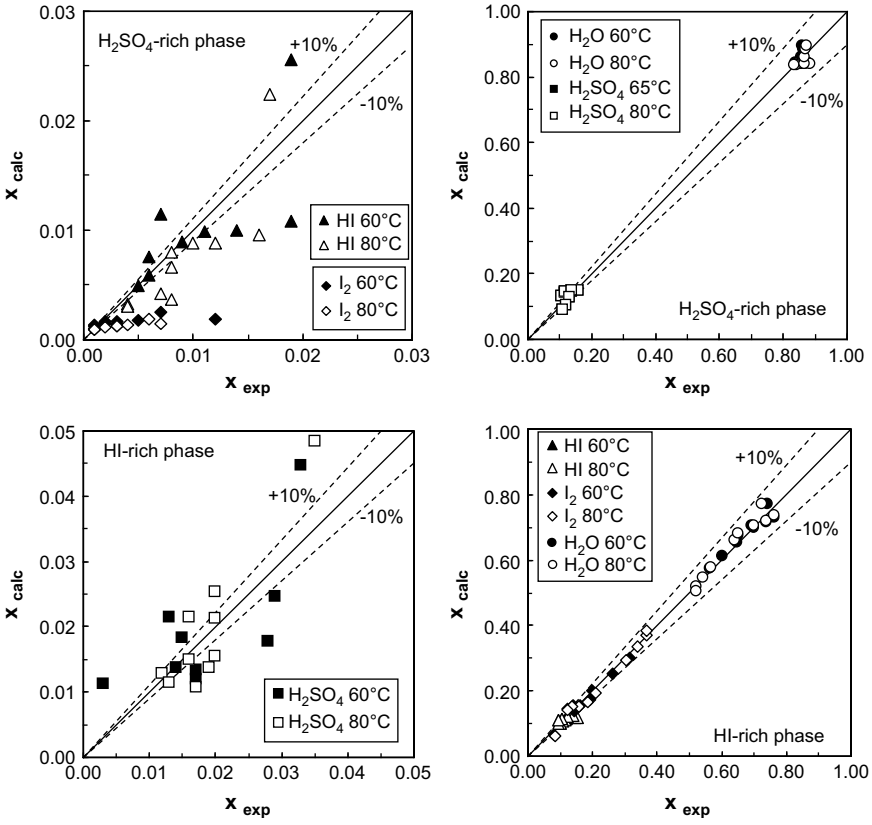


**Fig. 3 – Comparison of experimental and calculated values for Korean data points at 60 °C and 80 °C reported in Lee et al. [24].**

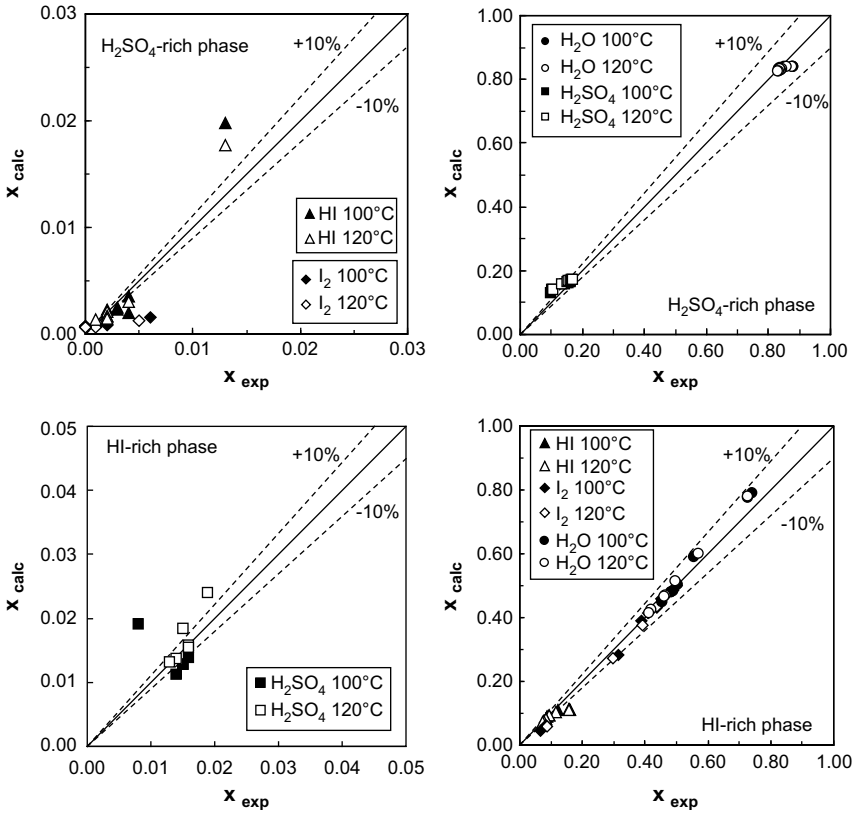


**Fig. 4 – Comparison of experimental and calculated values for Korean data points at 100 °C and 120 °C reported in Lee et al. [24].**

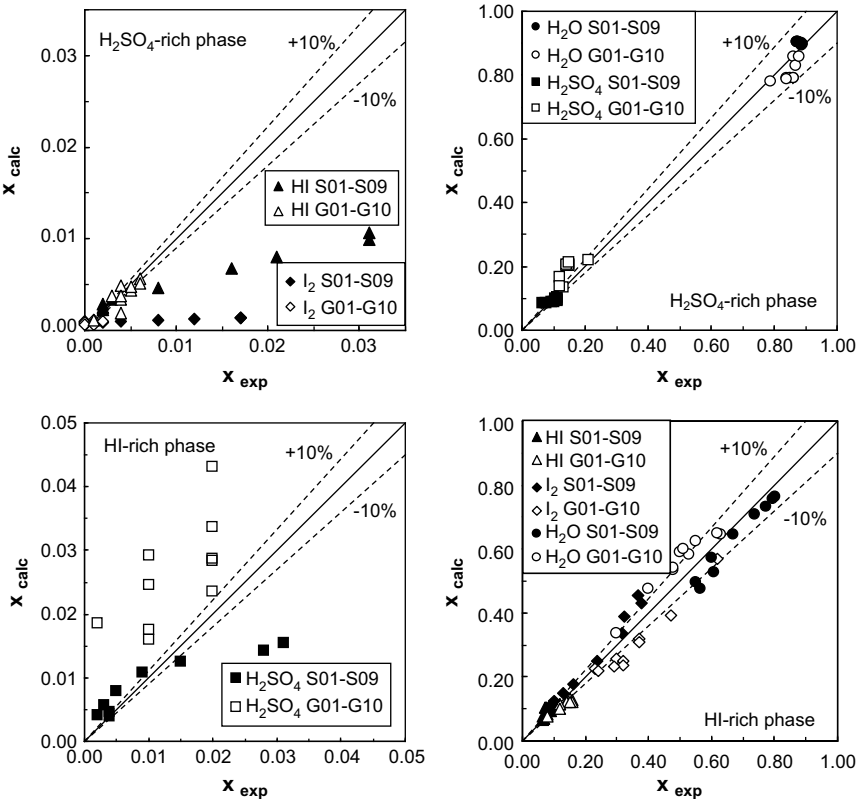


**Fig. 5 – Comparison of experimental and calculated values for data points of Sakurai (S01–S09) and Giaconia (G01–G10) reported in Lee et al. [24].**

not concern HI at 40 °C except that, if we assume that the model is correct, it may hint at some systematic deviation of the experimental data at 25 °C (no information about the accuracy was given in [24]).

At 60 and 80 °C, there is still a systematic underestimation of $I_2$ in the $H_2SO_4$-rich phase. For the other molar fractions, in particular for the other impurities in both phases, a scattering of the errors is observed. That could also indicate a scattering of the experimental data and hint at the experimental accuracy of these measurements.

At 100 °C and 120 °C, $I_2$ is again underestimated in the $H_2SO_4$-rich phase.

Overall, water is well predicted in the $H_2SO_4$-rich phase, which suggests the pertinence of the hypothesis the $H_2O$–$H_2SO_4$ mixtures (complete dissociation of the first acidity, hydration of the hydronium ion into $H_2SO_4$, $3H_2O$ and no interaction between water and $H_2SO_4$, $3H_2O$). The same holds for the water in the HI-rich phase.

#### 4.4.3. *Validation on Sakurai's and Giaconia's data points*

Regarding the data points of Sakurai (S01–S09 in [24]) and Giaconia (G01–G10 in [24]), the prediction bears the same remarks than for the Korean data but the errors are generally greater (see Table 3).

For the impurity $H_2SO_4$ in the HI rich phase in Giaconia's data points, the median relative error is much smaller than the mean relative error, indicating that unusually large errors, as confirmed by the very large maximum error of 494% (see Table 4). It corresponds to data point S08 where the $H_2SO_4$ molar fraction in the HI rich phase is the smallest (0.002) and of the order of magnitude of the experimental error reported by Giaconia et al. [23].

Experimental and calculated data values are displayed in Fig. 5 for the impurities and main component in the $H_2SO_4$-rich phase and in the in the HI-rich phase. +10% and −10% error lines are displayed for indication.

They show a trend of the model to underestimate the impurities $I_2$ and HI in the $H_2SO_4$-rich phase for Sakurai's data point and to overestimate the impurity $H_2SO_4$ in the HI-rich phase for Giaconia's points.

Overall, despite its achievements in representing the literature data and phase splitting, we may question the ability of the model to represent impurities, especially $I_2$ in the $H_2SO_4$-rich phase. However, before we remove some of the assumptions related to interactions neglected interactions, we would like to obtain accuracy information on all measurements, so as to evaluate the scattering of the measurements and their true accuracy. A current study progresses in this direction.

## 5. Conclusion

For the first time, a model for the Bunsen section of the Sulfur–Iodine thermo-chemical cycle is proposed, based on UNIQUAC's activity coefficient model combined with Engels' solvation model.

Real description of all species and phenomena is discussed but is not considered because of the complexity that it brings, in particular in terms of numerous model parameters. A simpler model is proposed after noticing that water excess versus the acids, hydrogen iodide and sulfuric acid, is always greater than 3. Therefore, we postulate the total dissociation of those acids and the complete hydration of the hydronium ion by 3 water molecules. That leads to the substitution of real HI and $H_2SO_4$ species by apparent [HI, $3H_2O$] and [$H_2SO_4$, $3H_2O$] species. Besides, to take into account the polyiodide ions formation that is strongly suspected, [HI, $3H_2O$] partial solvation by one $I_2$ molecule is described according to Engels' solvation model.

Furthermore, simplification hypotheses are proposed for the species interactions: the solvation complex of [HI, $3H_2O$] by $I_2$ is supposed to interact like $I_2$. and [$H_2SO_4$, $3H_2O$] is supposed to interact like $H_2O$. Reduction of the number of parameters with temperature dependency is significant and enables to reproduce phase splitting and to launch the parameter estimation procedure.

Lee et al. (2008) compiled 50 Korean data as well as Sakurai et al. (1999, 2000) 9 data points and Giaconia et al. (2007) 10 data points into a comprehensive table. 45 Korean points with $nI_2/nH_2SO_4 > 1$ are used in the estimation procedure using a relative error criterion. Other points and Kang et al. (2006)'s four non demixing points are used as validation.

The model reproduces all data and their demixtion with a mean relative error of 17.1% on the Korean points, below 6% for the main species (water and sulfuric acid in the $H_2SO_4$-rich phase; water, iodine and hydrogen iodide in the HI rich phase) and below 30% for the impurity species (iodine and hydrogen iodide in the $H_2SO_4$-rich phase; sulfuric acid in the HI rich phase).

For validation, Sakurai, Giaconia and kang data point are well predicted, but with larger errors than for the Korean points.

Better information on the scattering of the measurements and their true accuracy is needed to improve the model.

## REFERENCES

[1] Funk JE. Thermochemical hydrogen production: past and present. Int J Hydrogen Energy 2001;26(3):185–90.
[2] O'Keefe D, Allen C, Besenbruch G, Brown L, Norman J, Sharp R, et al. Preliminary results from bench-scale testing of a sulfur–iodine thermochemical water-splitting cycle. Int J Hydrogen Energy 1982;7(5):381–92.
[3] Mathias PM. Applied thermodynamics in chemical technology: current practice and future challenges. Fluid Phase Equilibria 2005;228–229:49–57.
[4] Hadj-Kali MK, Gerbaud V, Borgard JM, Baudouin O, Floquet P, Joulia X, et al. $HI_x$ system thermodynamic model for hydrogen production by the sulfur–iodine cycle. Int J Hydrogen Energy 2009;34:1696–709.
[5] Brown LC, Mathias PM, Chen CC, Ramrus D. Thermodynamic model for the HI–$I_2$–$H_2O$ system. AIChE Annual Meeting, 4–9 November, 2001.
[6] Mathias PM, Brown LC. Thermodynamics of the sulphur–iodine cycle for thermochemical hydrogen production. Presented at 68th Annual Meeting of the Society of Chemical Engineers, Japan, 2003.
[7] Annesini MC, Gironi F, Lanchi M, Marrelli L, Maschietti M. S–I thermochemical cycle for $H_2$ production: a thermodynamic

analysis of the phase equilibria of the system HI–$I_2$–$H_2O$. Proceedings of ICheaP-8, The eight Italian Conference on Chemical and Process Engineering, 2007.
[8] Roth M, Knoche KF. Thermo-chemical water-splitting through direct HI decomposition from HI/$I_2$/$H_2O$ solutions. Int J Hydrogen Energy 1989;14(8):545–9.
[9] Goldstein S, Borgard JM, Vitart X. Upper bound and best estimate of the efficiency of the iodine sulfur cycle. Int J Hydrogen Energy 2005;30(6):619–28.
[10] Belaissaoui B, Thery R, Meyer XM, Meyer M, Gerbaud V, Joulia X. Vapour reactive distillation process for hydrogen production by HI decomposition from HI–$I_2$–$H_2O$ solutions. Chem Eng Proc 2008;47(3):396–407.
[11] Neumann D. Phasengleichgewichte von HJ/$H_2O$/$J_2$ – Lösungen. Lehrstuhl für Thermodynamik, RWTH Aachen, 5100 Aachen (Germany). Master's thesis, January 1987.
[12] Yoon HJ, Kim SJ, No HC, Lee BJ, Kim ES. A thermo-physical model for hydrogen–iodide vapor–liquid equilibrium and decomposition behavior in the iodine–sulfur thermo-chemical water splitting cycle. Int J Hydrogen Energy 2008;33(20):5469–76.
[13] Palmer AD, Lietzke MH. The equilibria and kinetics of iodine hydrolysis. Radiochim Acta 1982;31:37–44.
[14] Palmer AD, Ramette RW, Mesmer RE. Triiodide ion formation equilibrium and activity coefficients in aqueous solution. J Solution Chem 1984;13(9):673–83.
[15] Calabrese VT, Khan A. Polyiodine and polyiodide species in an aqueous solution of iodine + KI: theoretical and experimental studies. J Phys Chem A 2000;104:1287–92.
[16] Elder RH, Priestman GH, Ewan BC, Allen RWK. The separation of HIx in the sulphur–iodine thermochemical cycle for sustainable hydrogen production. Trans IChemE, Part B 2005;7:343–50.
[17] Normann JH, Besenbuch GE, Brown LC. Thermo-chemical water-splitting cycle. Bench scale investigations and process engineering. DOE/ET/26225, 1981.
[18] Kracek FC. Solubilities in the system water–iodine to 200 °C. J Phys Chem 1931;35:417–22.
[19] Sakurai M, Nakajima H, Rusli A, Onuki K, Shimizu S. Experimental study on side-reaction occurrence condition in the sulfur–iodine thermochemical hydrogen production process. Int J Hydrogen Energy 2000;25:613–9.
[20] Sakurai M, Nakajima H, Onuki K, Ikenoya K, Shimizu S. Preliminary process analysis for the closed cycle operation of the iodine–sulfur thermochemical hydrogen production process. Int J Hydrogen Energy 1999;24:603–12.
[21] Sakurai M, Nakajima H, Onuki K, Shimizu S. Investigation of 2 liquid phase separation characteristics on the sulfur–iodine thermochemical hydrogen production process. Int J Hydrogen Energy 2000;25:605–11.
[22] Kang YH, Ryu JC, Park CS, Hwang GJ, Lee SH, Bae KK, et al. The study on Bunsen reaction process for iodine–sulfur thermochemical hydrogen production. Korean Chem Eng Res 2006;44(4):410–6.
[23] Giaconia A, Caputo G, Ceroli A, Diamanti M, Barbarossa V, Tarquini P, et al. Experimental study of two phase separation in the Bunsen section of the sulfur–iodine thermochemical cycle. Int J Hydrogen Energy 2007;32:531–6.
[24] Lee BJ, No HC, Yoon HJ, Kim SJ, Kim ES. An optimal operating window for the Bunsen process in the S–I thermochemical cycle. Int J Hydrogen Energy 2008;33:2200–10.
[25] Davis ME, Conger WL. An entropy production and efficiency analysis of the Bunsen reaction in the general atomics sulfur–iodine thermochemical hydrogen production cycle. Int J Hydrogen Energy 1980;5:475–85.
[26] Mathias PM. Modeling the sulfur–iodine cycle: Aspen Plus building blocks and simulation models. Report GA and Sandia National Laboratories; 2002.
[27] Chen CC, Britt HI, Boston JF, Evans LB. Local composition model for excess Gibbs energy of electrolyte systems. Part I: single solvent, single completely dissociated electrolyte systems. AIChE J 1982;28:588–96.
[28] Chen CC, Evans LB. A local composition model for the excess Gibbs energy of aqueous electrolyte systems. AIChE J 1986;32: 444–54.
[29] Pitzer K. Electrolytes. From dilute solutions to fused salts. J Am Chem Soc 1980;102:2902–6.
[30] Renon H, Prausnitz JM. Local compositions in thermodynamic excess functions for liquid mixtures. AIChE J 1968;14(3):135–44.
[31] O'Connell J. Oral Conference at ESAT (29/05/2008–01/06/ 2008), Cannes, France, 2008.
[32] Zemaïtis JF, Clark DM, Marshall R, Scrivner NC. Handbook of aqueous electrolyte thermodynamics: theory & application. Editions DIPPR; 1986.
[33] Chen CC, Mathias PM, Orbey H. Use of hydration and dissociation chemistries with the electrolyte-NRTL model. AIChE J 1999;45(7):1576–86.
[34] Anderson TF, Prausnitz JM. Application of the UNIQUAC Equation to Calculation of Multicomponent Phase Equilibria. 1. Vapor–Liquid Equilibria. Ind Eng Chem Process Des Dev 1978;17(4):552–61.
[35] Bondi A. van der Waals volumes and radii. J Phys Chem 1964; 68:441–51.
[36] Abrams DS, Prausnitz JM. Statistical thermodynamics of liquid mixtures: a new expression for the excess Gibbs energy of partly or completely miscible systems. AIChE J 1975;21(3):116–28.
[37] Engels H. Phase equilibria and phase diagrams of electrolytes. In: Chemistry data series, vol. XI. DECHEMA; 1990. Part I.
[38] Pickering SE. Die Hydrate der Jodwasserstoffsäure. 1893; 2307–10.
[39] Zavitsas AA. Properties of water solutions of electrolytes and nonelectrolytes. J Phys Chem B 2001;105:7805–15.
[40] ProSim, Simulis®. Thermodynamics user guide, http://www.prosim.net; 2004.